Simulation of Methane Partial Oxidation over Silica-Supported MoO_3 and V_2O_5

Michael D. Amiridis, James E. Rekoske, James A. Dumesic, and Dale F. Rudd
Dept. of Chemical Engineering, University of Wisconsin, Madison, WI 53706

Nicholas D. Spencer and Carmo J. Pereira
Research Div., W. R. Grace and Co., Columbia, MD 21044

Microkinetic simulations have been carried out to describe the partial oxidation of methane over silica-supported molybdena and vanadia. The objective of this study was to formulate a physically reasonable reaction network to capture the basic aspects of the surface catalytic chemistry and to use this network to link methane oxidation kinetics with the kinetics observed for the oxidation of subsequent gaseous products, i.e., methanol, formaldehyde, and carbon monoxide. The most abundant reactive intermediates on the catalyst surface are suggested to be oxygen and hydroxyl groups. This reaction network successfully predicts the catalytic activities, selectivities, activation energies, and reaction orders observed over silica-supported molybdena and vanadia; and the microkinetic model also semiquantitatively explains the kinetic trends for related catalyst systems and is consistent with surface bonding energetics reported in the literature over various oxide catalysts. The microkinetic reaction network properly reduces to the more simple macrokinetic model reported previously for methane partial oxidation.

Introduction

Because of its high natural abundance and low cost, methane is an attractive source of chemical compounds and its activation is currently an area of extensive research. Although the partial oxidation of methane to methanol and formaldehyde is a thermodynamically favorable process, severe conditions are required to activate the otherwise stable methane molecule. Under such conditions, however, the oxygenated species are oxidized to carbon dioxide and water.

In current industrial practice, methanol is produced from methane by steam reforming followed by methanol synthesis from CO and H_2 (Van Hook, 1980; Klier, 1982). In a subsequent step, methanol is further oxidized to formaldehyde (Sperber, 1969; Pernicone et al., 1969). The energetics of the sequence are such that a direct route from methane to formaldehyde would be attractive from an economic point of view.

Several catalysts for such a reaction have been studied in the literature, with most of the attention being focused on molybdenum-based systems. High selectivities toward the desired products are usually achieved at low methane conversion levels. Higher selectivities (up to 90%) have been reported (Khan and Somorjai, 1985) when nitrous oxide (N_2O) is used as the oxidizing agent. The high cost of nitrous oxide, however, makes this option economically unattractive.

Spencer and Pereira (Spencer, 1988; Spencer and Pereira, 1987, 1989) have studied the partial oxidation of methane by molecular oxygen over molybdenum and vanadium oxides supported on silica. They found both catalysts to be active and selective for the reaction. They also developed a first-order kinetic model which, by the use of different parameters and a slightly altered mechanism, successfully described the kinetic data for both systems.

In this article, we apply microkinetic simulation techniques to describe the oxidation of methane, methanol, formaldehyde and carbon monoxide over silica-supported molybdena and vanadia. The strategy of this approach is to employ a simple reaction mechanism to capture the basic chemistry taking place

Correspondence concerning this article should be addressed to J. A. Dumesic.

on the catalyst surface and to use this mechanism in an attempt to coordinate and extrapolate diverse experimental studies. For the case of methane activation, we require that the microkinetic simulation must:

- Describe the steady-state kinetics over a wide range of reaction conditions
- Utilize reactive intermediates that have been observed spectroscopically or are chemically reasonable
- Employ surface thermodynamic and kinetic parameters that can be measured independently or that can be estimated by theories of chemical bonding
- Reproduce the kinetic behavior of other catalytic processes that can be constructed from a subset of the elementary steps used in the larger simulation.

It is important to note that microkinetic simulations can be carried out at different levels of detail, depending on the availability of surface kinetic, thermodynamic, spectroscopic and structural information. At one end of the spectrum are cases where the nature, bonding and reactivity of reactants, products and principal intermediates involved in the catalytic process have been determined by surface science studies on different single crystals and by kinetic, chemical and spectroscopic studies on a variety of high surface area catalytic materials. At the other end of the spectrum are cases where kinetic data are available but where surface science and spectroscopic data are limited. This case of methane activation appears near the latter end of the spectrum. To be effective in this case, the mechanism used in microkinetic simulations need not be accurate in detail. Instead, we attempt to incorporate at least some of the essential surface catalytic chemistry into the kinetic model, with the hope that this model will be more successful than a simple first-order model for generalizing and extrapolating kinetic results for methane activation, as well as the oxidation of methanol, formaldehyde and carbon monoxide.

Finally, we compare the results of our microkinetic model and the first-order macrokinetic model previously proposed for the same reactions by Spencer and Pereira. We show that the more general microkinetic model can be reduced to the macrokinetic model under specific conditions, and we discuss the applicability and the advantages of each approach.

General Mechanism for Methane Oxidation

The oxidation of methane results primarily in the formation of formaldehyde, carbon monoxide, carbon dioxide and water. Although methanol is produced only in trace amounts, it is believed to be an important intermediate.

As mentioned above, Spencer and Pereira utilized the results of several kinetic studies over MoO_3/SiO_2 and V_2O_5/SiO_2 to suggest a reaction network that leads to the formation of these products. After examining the product distribution of methane oxidation near zero conversion, as well as the product distributions of formaldehyde and methanol oxidations, they suggested the existence of two alternative pathways: one leading directly to the formation of CO_2 and the other to the formation of HCHO and its subsequent oxidation to CO and CO_2. From their kinetic simulations they also concluded that both pathways follow a common initial methane activation step.

Following the aforementioned ideas, a possible mechanism for methane partial oxidation over supported metal oxides is suggested as follows:

$$CH_4 + 2MO \rightleftharpoons MOCH_3 + MOH \quad (1)$$

$$MOCH_3 + MO \rightleftharpoons MOCH_2 + MOH \quad (2)$$

$$MOCH_2 \rightleftharpoons HCHO + M \quad (3)$$

$$HCHO + MO \rightleftharpoons MOCH_2O \quad (4)$$

$$MOCH_2O + MO \rightleftharpoons CO + 2MOH \quad (5)$$

$$2MOH \rightleftharpoons H_2O + MO + M \quad (6)$$

$$2M + O_2 \rightleftharpoons 2MO \quad (7)$$

$$MOCH_3 + 2MO \rightleftharpoons MOCH_2OM + MOH \quad (8)$$

$$MOCH_2OM + 2MO \rightleftharpoons CO_2 + 2MOH + 2M \quad (9)$$

$$MOCH_3 + MOH \rightleftharpoons CH_3OH + MO + M \quad (10)$$

$$CO + MO \rightleftharpoons MCO_2 \quad (11)$$

$$MCO_2 \rightleftharpoons CO_2 + M \quad (12)$$

Steps 8 and 9 represent the direct CO_2 formation pathway of Spencer and Pereira, steps 2–5, 11 and 12 represent the HCHO pathway, and step 1 is the common methane activation reaction. Steps 6 and 10 account for the desorption of water and methanol from the surface, while step 7 represents the surface reoxidation. Figure 1 represents the above mechanism where one can distinguish different pathways. For simplicity, the active sites (*MO* and *M*), as well as the hydroxyl groups, are not included in this figure.

While the proposed mechanism is not necessarily accurate in detail, it appears to agree with most of the existing literature. The presence of the methoxy species on oxidized surfaces following methane and methanol adsorption has been documented by the use of *in situ* infrared spectroscopy (Edwards et al., 1977; Machiels and Sleight, 1982; Chung et al., 1988;

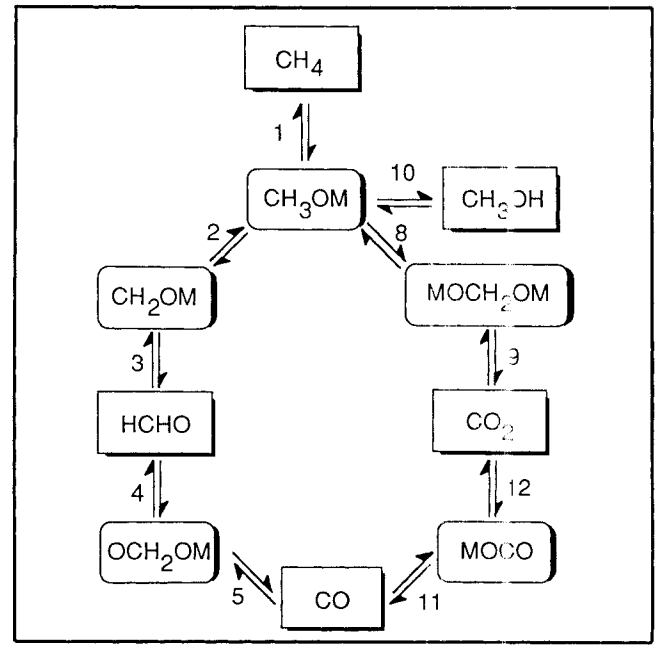

Figure 1. General mechanism for methane partial oxidation over supported metal oxides.

Chung and Bennett, 1985; Feil et al., 1987; Busca, 1989) and EPR spectroscopy (Kaliaguine et al., 1978). There is also evidence for the presence of formaldehyde, weakly adsorbed on a reduced metal site (Feil et al., 1987; Busca, 1989), as well as a CH_2 species bonded to two surface oxygens (Machiels and Sleight, 1982; Feil et al., 1987; Busca, 1989), although the nature and the role of this latter intermediate has not been determined. We have elected to treat the $MOCH_2O$ species as a weakly adsorbed formaldehyde on an oxidized site, although the possibility of a biformate species should not be ruled out. In such a case, the heat of formation of this species would differ by approximately 10%. Our overall scheme is also in general agreement with mechanisms proposed by Dowden et al. (1968), Feil et al. (1987), and Busca (1989). Finally, it is important to note that we have not made any assumptions about the existence of rate-determining steps or most abundant surface intermediates.

Formulation of the Microkinetic Model

The rate constants for each elementary reaction were estimated following the method outlined previously (Goddard et al., 1989). The preexponential factors for the adsorption of gaseous species were estimated to be approximately 1.2×10^3 $Pa^{-1} \cdot s^{-1}$, assuming that the surface species were immobile. Different values were used, however, for step 1 (the adsorption of methane). Specifically, these higher values (1.4×10^5 $Pa^{-1} \cdot s^{-1}$ over MoO_3 and 3.7×10^6 $Pa^{-1} \cdot s^{-1}$ over V_2O_5) were required to correctly describe the activity vs. temperature behavior of the two catalysts. It is possible that step 1 of our mechanism is a combination of two elementary steps in reality. The initial formation, for example, of a precursor state on the surface and its consecutive dissociation to form a methoxy and hydroxyl group. Another possible combination would be the activation of a surface oxygen atom to O^-, which accommodates the methoxy species, and the consecutive dissociative adsorption of methane. In any case, such a combination could justify the higher than typical preexponential factors used for step 1 in our simulations.

For reactions involving only adsorbed species and for desorption processes, the preexponential factors were estimated to be 10^{13} s^{-1}. However, depending on the extent of surface mobility of the intermediates, as well as their rotational freedom, the preexponential factors could vary by three orders of magnitude. A lower preexponential factor was used for the desorption of water ($1.4 \times 10^{12} s^{-1}$) so that our model could better describe the inhibiting effect of water on the oxidation of methane. Different preexponential factors were also used for the forward and reverse reactions of step 2, the dehydrogenation of surface methoxy species to give metal-bonded formaldehyde ($1.7 \times 10^{16} s^{-1}$) and the forward reaction of step 5, the oxidation of adsorbed formaldehyde to CO (2.3×10^8 s^{-1} for V_2O_5 and 8.2×10^{10} s^{-1} for MoO_3), which is a combination of several elementary steps and hence the lower value can be justified. Finally, we should mention that although reactions 8 and 9 appear to be three body reactions, the high availability of oxygen on the surface (species $M=O$) makes these steps possible, and the preexponential factor of 10^{13} s^{-1} is reasonable.

The heat of each elementary reaction was estimated using heats of formation of the species involved. For each species, an estimation of the gaseous heat of formation was obtained from the literature and this value was converted to a surface heat of formation by using the strength of its bond with the surface. Finally, the activation energy was calculated assuming that it is a linear function of the heat of reaction, according to the Polanyi expression:

$$E_{A_i} = E_0 + \alpha \Delta H_i \tag{13}$$

The value of 0.5 was assigned to the parameter α. The values of E_0 were obtained by an optimization process that minimized the deviations of the model predictions from the experimental data. The results indicated high values of E_0 for the adsorption of methane and the consecutive oxidation of formaldehyde to CO and CO_2 (steps 1, 5, 11 and 12). The value of E_0 used for the dehydrogenation of CH_3 to CH_2 (step 2) was comparable to the one used in ethane hydrogenolysis (Goddard et al., 1989), while lower values were used for the remaining steps. The results are shown in Table 1.

Table 1. E_0 Parameters Used in Simulations

Step	MoO_3/SiO_2 kJ·mol^{-1}	V_2O_5/SiO_2 kJ·mol^{-1}
1	243	264
2	117	117
3,4,6,7,8,9	42	42
5	230	188
11,12	188	188
10	63	63

The chemical bonding parameters used in our simulations to estimate the heat of formation of the surface species are shown in Table 2. Initially, a range for each of the parameters was estimated from the existing literature, as explained in detail below. The same optimization process was then followed, as in the case of the values of the Polanyi constants (E_0), to determine the best value within this range.

If one knows the heat of adsorption of O_2 (Q_{O_2}), the strength of the bond between atomic oxygen and a surface metal atom ($M=O$) can be determined from the relation:

$$M=O = \frac{D_{O_2} - Q_{O_2}}{2}, \tag{14}$$

where D_{O_2} is the gas-phase dissociation energy of O_2 (498 kJ·mol^{-1}). Stradella and Vogliolo (1983) have determined the integral molar heat of adsorption of dioxygen over reduced

Table 2. Bonding Energies Used in Simulations

Bond	MoO_3/SiO_2 kJ·mol^{-1}	V_2O_5/SiO_2 kJ·mol^{-1}
M=O	384	346
M-OH	293	256
M-OCH_3	248	234
M-OCH_2	84	126
MO-CH_2O	21	40
MO-CO	84	111

$Bi_2O_3 \cdot MoO_3$ to be 297 kJ·mol^{-1}. Therefore, one can estimate the $M=O$ parameter to be 398 kJ·mol^{-1} for MoO_3, given that the presence of Bi_2O_3 at a Bi_2O_3/MoO_3 ratio of 1 does not appear to effect the energetics of O bonding, as demonstrated by Klissurski (1979). One can also use the value of 313 kJ·mol^{-1} for the heat of adsorption of oxygen reported by Krivanek and coworkers (1971) to calculate the $M=O$ parameter at 405 kJ·mol^{-1}. The $M=O$ value used in our kinetic simulations for MoO_3 was 384 kJ·mol^{-1}, and it appears to be in good agreement with the existing literature.

Muzykantov and coworkers (1968) determined the rate of the oxygen desorption at 808 K over V_2O_5 by the use of isotope exchange. Assuming a site density of 10^{19} sites/m^2 and a preexponential factor of 10^{13} s^{-1} for the desorption process, one can estimate an activation energy of 230 kJ·mol^{-1}, which can be assumed to be equal to the heat of adsorption since the adsorption is a highly exothermic process. Equation 14 can then be applied and results in an $M=O$ value for V_2O_5 of 364 kJ·mol^{-1}. Pankratiev and coworkers (1985) determined calorimetrically the heat of adsorption of O_2 on a 70 mol % V_2O_5, 30 mol % MoO_3 sample. Their result of 250 kJ·mol^{-1} is in good agreement with the previous calculations and provides an $M=O$ value for V_2O_5 of 374 kJ·mol^{-1}. In our kinetic simulations, we used an $M=O$ value of 346 kJ·mol^{-1} for V_2O_5, which is in good agreement with the existing literature.

One can estimate the strength of the bond between hydroxyl groups and surface (M-OH) from the heat of adsorption of water, using the above strength of the $M=O$ bond as illustrated below. From the gas-phase dissociation energy of H_2, one can calculate the heat of formation of H to be 218 kJ/mol. Similarly, the heat of formation of O can be calculated to be equal to 249 kJ/mol. Further, from the strength of the bond between the hydrogen atom and the hydroxyl group in water, the heat of formation of the OH group can be calculated to be 39 kJ/mol.

Finally, from the adsorption of water

$$H_2O + M + MO \rightarrow 2MOH \qquad (15)$$

one has

$$\Delta H_{ads} = 2H_{f,MOH} - H_{f,H_2O} - H_{f,M} - H_{f,MO} \qquad (16)$$

where the heats of formation of the surface species can be calculated from the heats of formation of the corresponding gaseous species by use of the corresponding surface bonds [i.e., $H_{f,MOH} = H_{f,O} - (M-OH)$].

Stradella and Vogliolo (1983) measured the heat of adsorption of water to be 200 kJ·mol^{-1} on either reduced or oxidized $Bi_2O_3 \cdot MoO_3$, which corresponds to an M-OH value of 327 kJ·mol^{-1}. Bond order conservation (BOC) calculations (Shustorovich, 1986) can also be employed to provide an estimate of M-OH, given the value of $M=O$. Such calculations indicate the M-OH parameter to be between 75% and 80% of $M=O$. In our simulations, the values of 293 and 256 kJ·mol^{-1} were used for the M-OH parameter for MoO_3 and V_2O_5, respectively, which correspond to approximately 75% of the $M=O$ parameters used for the same catalysts.

Temperature-programmed desorption experiments performed by Chung and coworkers (1985) suggest that hydroxyl groups are bonded more strongly to a molybdenum oxide surface than methoxy groups. From temperature-programmed reaction spectroscopy experiments performed by Ko and Madix (1981) on a Mo(100)-(1×1)O surface, one can estimate the heat of adsorption of methanol to be roughly 96 kJ·mol^{-1} by using the peak temperature of 370 K and a normal preexponential factor of 10^{13}s^{-1}, which corresponds to an M-OCH_3 value of 255 kJ·mol^{-1}. In our kinetic simulations, the values of 248 and 234 kJ·mol^{-1} were used for the M-OCH_3 parameter for MoO_3 and V_2O_5, respectively, corresponding to heats of adsorption of methanol of approximately 88 and 75 kJ·mol^{-1} on these catalysts.

Our microkinetic model includes two types of formaldehyde present on the catalyst surface, namely formaldehyde bonded on a reduced or on an oxidized site. Chemical intuition would suggest that the surface bond energies for these species would be substantially lower than the values described above for other species, since all of the atoms in formaldehyde are electronically saturated. Thus, for the M-OCH_2 parameter, we used the values of 84 and 126 kJ·mol^{-1} for MoO_3 and V_2O_5, respectively, while for the MO-CH_2O parameter, we used values below 42 kJ·mol^{-1}.

The heat of adsorption of CO on metal oxides is usually lower than 63 kJ·mol^{-1}. Based on such an assumption one can estimate the MO-CO parameter of our model to be between 63 and 126 kJ·mol^{-1}. The values of 84 and 111 kJ·mol^{-1} were used for MoO_3 and V_2O_5 in our simulations respectively.

Finally, it should be mentioned that for the multiple-bonded $MOCH_2OM$ species the strength of the surface bonds was assumed to be similar to that of the methoxy groups and the M-OCH_3 parameter was used.

The preexponential factors and the activation energies for each elementary step, resulting from the calculations explained in detail above, are given in Tables 3 and 4 for both MoO_3 and V_2O_5. A sensitivity analysis was performed by changing each individual rate constant by 10% and examining the effects that such a change had on the overall rate as well as the product distribution. It was observed that, from the 24 kinetic rate constants, only a few are kinetically significant and need to be estimated. In the case of MoO_3, for example and under methane oxidation conditions, steps 3, 6, 7 and 9 appear to be kinetically-insignificant, while steps 10-12 occur only at a very low rate and do not influence neither the methane conversion nor the product distribution. Furthermore, step 4 is suggested to be essentially at equilibrium, while steps 1, 2, 5 and 8 are suggested to be irreversible. Therefore, only five constants become kinetically-significant and need to be estimated: K_4, k_1, k_2, k_5, k_8 (where K_i and k_i are equilibrium and rate constants for step i, respectively).

Similarly, for V_2O_5 under methane oxidation conditions, steps 2, 3, 6, 7 and 12 appear to be kinetically-insignificant, while steps 8–10 are negligible. Furthermore, with step 4 being in equilibrium and steps 1, 5 and 11 being irreversible, only four constants are important and need to be estimated: K_4, k_1, k_5, k_{11}.

In general, the kinetic network of this study can be parameterized in different ways. We have decided to use the strengths of the bonds between the surface and the adsorbed species as our parameters, not individual rate constants. In this way, we feel that we can better capture the essential surface chemistry. In addition to being physically meaningful, each of

Table 3. Preexponential Factors and Activation Energies of Elementary Steps for Simulations over MoO_3/SiO_2

Step	Preexponential Factors		Activation Energies (kJ/mol)	
	Forward	Reverse	Forward	Reverse
1	1.4×10^{5} Pa$^{-1}\cdot$s^{-1}*	1.1×10^{13} s^{-1}	204*	282
2	1.7×10^{16} s^{-1}*	1.7×10^{16} s^{-1}	42*	193
3	1.1×10^{13} s^{-1}	1.1×10^{0} Pa$^{-1}\cdot$s^{-1}	84	0
4	1.2×10^{3} Pa$^{-1}\cdot$s^{-1}*	1.1×10^{13} s^{-1}*	31*	52*
5	8.2×10^{10} s^{-1}*	1.2×10^{3} Pa$^{-1}\cdot$s^{-1}	124*	337
6	1.4×10^{12} s^{-1}	1.2×10^{3} Pa$^{-1}\cdot$s^{-1}	131	0
7	1.2×10^{3} Pa$^{-1}\cdot$s^{-1}	1.1×10^{13} s^{-1}	0	269
8	1.1×10^{13} s^{-1}*	1.1×10^{13} s^{-1}	0*	179
9	1.1×10^{13} s^{-1}	1.2×10^{3} Pa$^{-1}\cdot$s^{-1}	0	271
10	1.1×10^{13} s^{-1}	1.7×10^{2} Pa$^{-1}\cdot$s^{-1}	106	20
11	1.2×10^{3} Pa$^{-1}\cdot$s^{-1}	1.1×10^{13} s^{-1}	180	198
12	1.1×10^{13} s^{-1}	1.2×10^{3} Pa$^{-1}\cdot$s^{-1}	124	254

*Steps that are kinetically-significant under methane oxidation conditions.

Table 4. Preexponential Factors and Activation Energies of Elementary Steps for Simulations over V_2O_5/SiO_2

Step	Preexponential Factors		Activation Energies (kJ/mol)	
	Forward	Reverse	Forward	Reverse
1	3.7×10^{6} Pa$^{-1}\cdot$s^{-1}*	1.1×10^{13} s^{-1}	211*	317
2	1.7×10^{16} s^{-1}	1.7×10^{16} s^{-1}	13	222
3	1.1×10^{13} s^{-1}	1.1×10^{0} Pa$^{-1}\cdot$s^{-1}	126	0
4	1.2×10^{3} Pa$^{-1}\cdot$s^{-1}*	1.1×10^{13} s^{-1}*	22*	62*
5	2.3×10^{8} s^{-1}*	1.2×10^{3} Pa$^{-1}\cdot$s^{-1}	89*	288
6	1.4×10^{12} s^{-1}	1.2×10^{3} Pa$^{-1}\cdot$s^{-1}	97	0
7	1.2×10^{3} Pa$^{-1}\cdot$s^{-1}	1.1×10^{13} s^{-1}	0	190
8	1.1×10^{13} s^{-1}	1.1×10^{13} s^{-1}	0	207
9	1.1×10^{13} s^{-1}	1.2×10^{3} Pa$^{-1}\cdot$s^{-1}	0	303
10	1.1×10^{13} s^{-1}	1.2×10^{3} Pa$^{-1}\cdot$s^{-1}	100	25
11	1.2×10^{3} Pa$^{-1}\cdot$s^{-1}*	1.1×10^{13} s^{-1}	147*	231
12	1.1×10^{13} s^{-1}	1.2×10^{3} Pa$^{-1}\cdot$s^{-1}	137	240

*Steps that are kinetically-significant under methane oxidation conditions.

our parameters affects those elementary reactions that involve the same surface chemical bonds in a consistent manner. Finally, it should be pointed out that it is not the absolute values of our energetic parameters that are important, but rather the differences between them.

Quantitative Comparison: Kinetic Simulations vs. Experimental Data

The first objective of our kinetic modeling study was to simulate the data collected by Spencer and Pereira (Spencer, 1988; Spencer and Pereira, 1987, 1989) for methane oxidation over MoO_3 and V_2O_5 supported on SiO_2. These data have been reported in the form of product selectivity (the percentage of product based on converted methane) vs. methane conversion. The simulated selectivity vs. conversion curves for MoO_3/SiO_2 in a plug flow reactor are shown in Figures 2a-2c, compared with the experimental data at three temperatures. There is an excellent agreement at all temperatures. The same type of comparison is shown in Figures 3a-3c for V_2O_5/SiO_2.

The second requirement of the reaction network was that it could also simulate the methanol and formaldehyde oxidation experiments performed by these authors with similar success. Figure 4 shows model predictions for the product distribution of formaldehyde oxidation over MoO_3/SiO_2 at a temperature

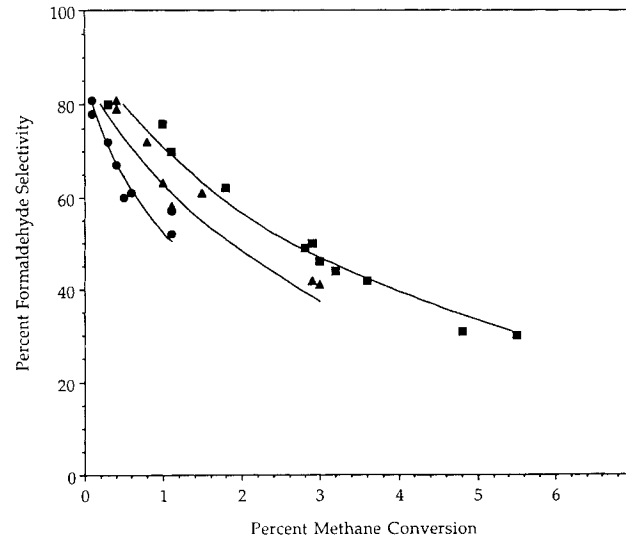

Figure 2a. Formaldehyde selectivity vs. methane conversion over MoO_3/SiO_2.

Experimental data at 848 K (●), 873 K (▲), and 898 K (■); model predictions (——). P_{tot} = 1 $\times 10^5$ Pa, 9:1 methane to oxygen molar ratio.

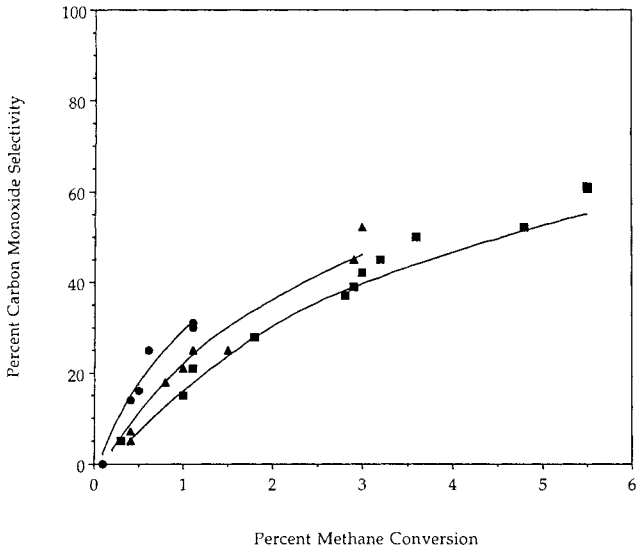

Figure 2b. Carbon monoxide selectivity vs. methane conversion over MoO_3/SiO_2.

Experimental data at 848 K (●), 873 K (▲), and 898 K (■); model predictions (——). P_{tot} = 1 $\times 10^5$ Pa, 9:1 methane to oxygen molar ratio.

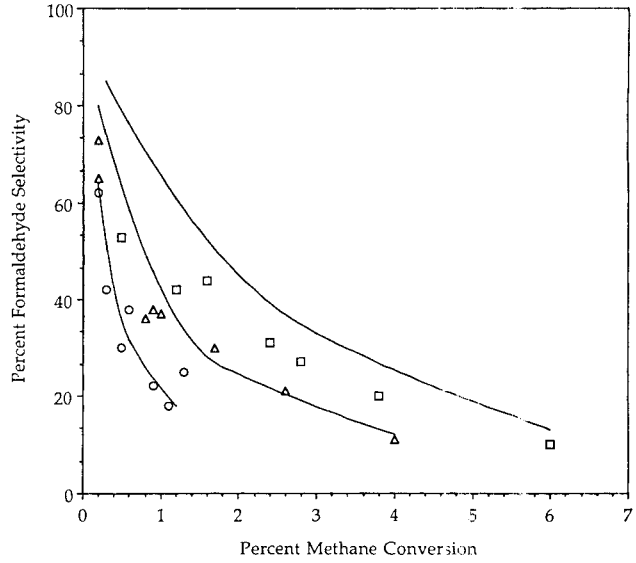

Figure 3a. Formaldehyde selectivity vs. methane conversion over V_2O_5/SiO_2.

Experimental data at 773 K (○), 798 K (△), and 823 K (□); model predictions (——). P_{tot} = 1 $\times 10^5$ Pa, 9:1 methane to oxygen molar ratio.

range between 600 and 925 K. As in the case of the experimental data, carbon monoxide is the principal product, with small amounts of carbon dioxide formed at higher temperature. The model predicts the catalytic activity to start at approximately 650 K with 50% formaldehyde conversion achieved near 855 K, both results are in agreement with the experimental data. The only discrepancy occurs in the amount of CO_2 produced at high temperature, where the model prediction appears to be lower than the experimental observation.

The product distribution predicted by the microkinetic model for methanol oxidation over MoO_3/SiO_2 at a temperature range between 500 and 900 K is shown in Figure 5. The model predicts the catalytic activity to start near 500 K with 100% conversion reached at around 700 K, both results are in agreement with the experimental data. Furthermore, the amount of formaldehyde produced is predicted to pass through a maximum near 700 K, while the amount of CO increases monotonically, as observed experimentally. The only discrepancy occurs in the amounts of CO and CO_2 produced, where the model predictions appear to be lower for CO and higher for CO_2.

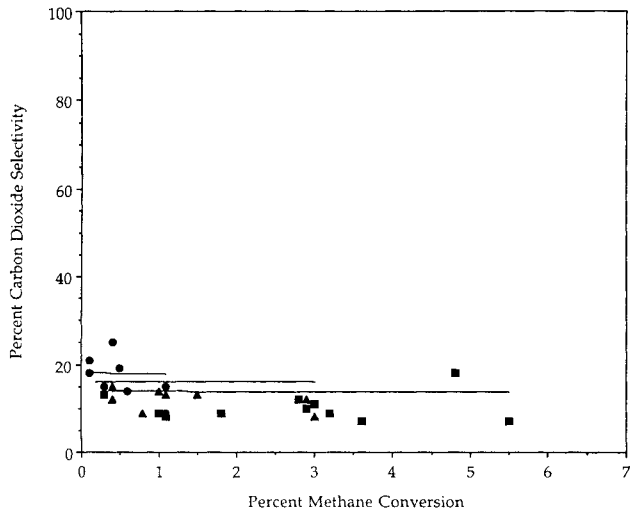

Figure 2c. Carbon dioxide selectivity vs. methane conversion over MoO_3/SiO_2.

Experimental data at 848 K (●), 873 K (▲), and 898 K (■); model predictions (——). P_{tot} = 1 $\times 10^5$ Pa, 9:1 methane to oxygen molar ratio.

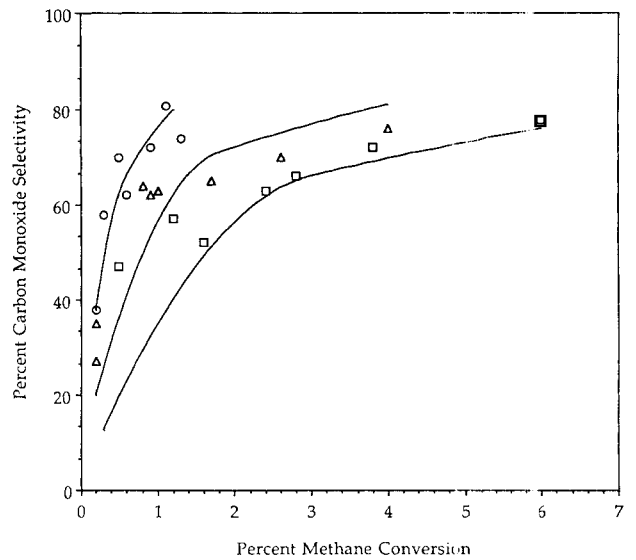

Figure 3b. Carbon monoxide selectivity vs. methane conversion over V_2O_5/SiO_2.

Experimental data at 773 K (○), 798 K (△), and 823 K (□); model predictions (——). P_{tot} = 1 $\times 10^5$ Pa, 9:1 methane to oxygen molar ratio.

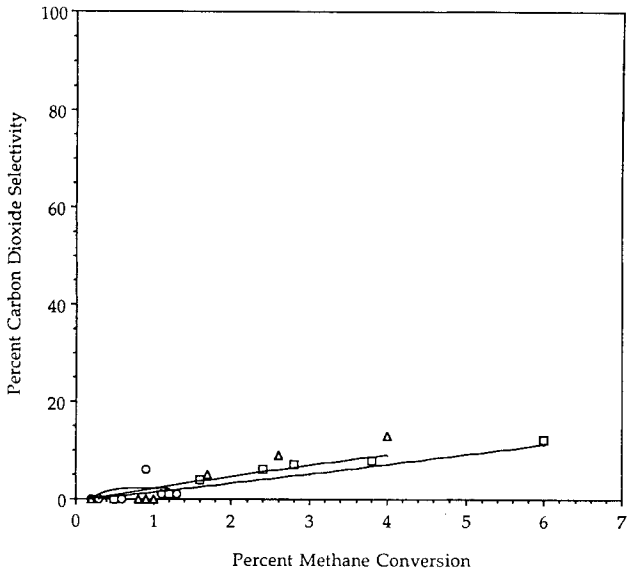

Figure 3c. Carbon dioxide selectivity vs. methane conversion over V_2O_5/SiO_2.

Experimental data at 773 K (○), 798 K (△), and 823 K (□); model predictions (——). P_{tot} = 1 $\times 10^5$ Pa, 9:1 methane to oxygen molar ratio.

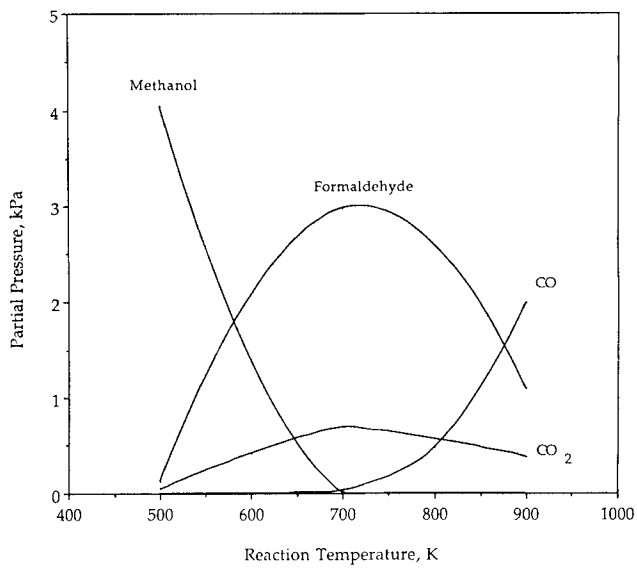

Figure 5. Model predictions for the product gas distribution during oxidation of 4.2 vol. % CH_3OH entrained in a 9:1 argon:oxygen mixture over MoO_3/SiO_2.

Simulations of formaldehyde oxidation over V_2O_5/SiO_2 between 500 and 900 K are shown in Figure 6. In agreement with the experimental data, a sigmoid curve represents the formaldehyde conversion. The model predicts the catalytic activity to start near 500 K, with 50% conversion reached at approximately 710 K and 100% conversion approached at about 900 K, all results in agreement with the experimentally observed values. Furthermore, the model predicts the CO production to pass through a maximum near 800 K and the CO_2 production to increase monotonically. Discrepancy again occurs in the amount of CO_2 produced at high temperatures, where the model predicted values higher than those observed experimentally.

The microkinetic model predicts that the only species present on the surface in any significant amounts under methane oxidation conditions are oxygen and hydroxyl groups. Under the above methane oxidation conditions, the hydroxyl surface concentration varies between 1% at the zero methane conversion

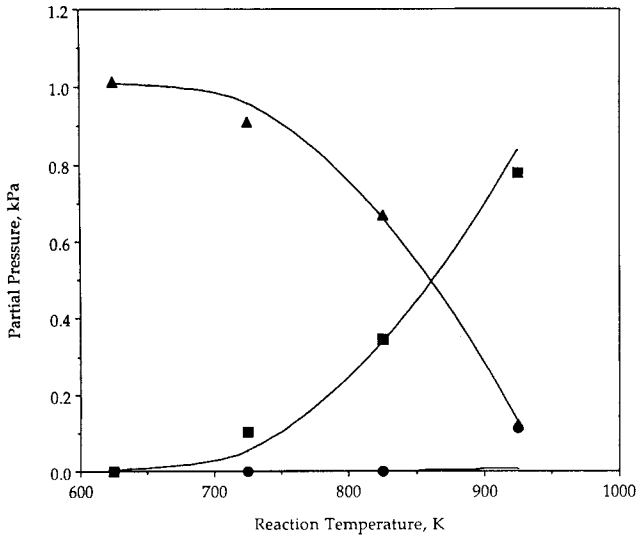

Figure 4. Product gas distribution during oxidation of 1 vol. % HCHO entrained in a 9:1 argon: oxygen mixture over MoO_3/SiO_2.

Experimental data for formaldehyde (▲), carbon monoxide (■), and carbon dioxide (●); model predictions (——).

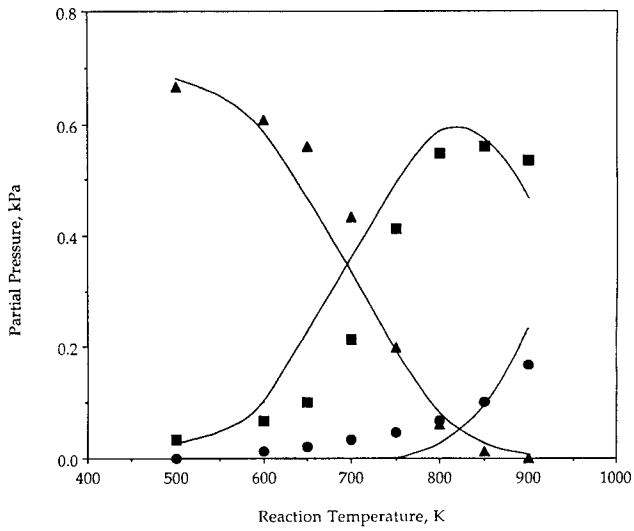

Figure 6. Product gas distribution during oxidation of 0.7 vol. % HCHO entrained in a 9:1 argon-:oxygen mixture over V_2O_5/SiO_2.

Experimental data for formaldehyde (▲), carbon monoxide (■), and carbon dioxide (●); model predictions (——).

limit and 15% at methane conversion levels around 7%, while under methanol oxidation conditions hydroxyl groups cover more than 90% of the surface. The concentration of hydroxyl groups present on the surface is controlled primarily by step 6 (water desorption) and this appears to have a significant effect on the kinetics of the system under different conditions, as discussed in the following section.

Qualitative Comparison: Kinetic Simulations vs. Related Experimental Data

We compare the predictions of the microkinetic model with experimental results of related experimental studies in the literature to test the validity of the model in different types of reactors and under conditions significantly different from those of Spencer and Pereira.

Cairati and coworkers (1982) studied the oxidation of methanol over MoO_3/SiO_2 in a fluidized-bed reactor. Using 5.5% methanol in air as the reactant mixture, they achieved 72% conversion of methanol at 588 K, with 76% selectivity toward formaldehyde. When the temperature was raised to 668 K, the conversion was almost complete (96%), while the selectivity toward formaldehyde decreased to 66%. In agreement with the experiments, the microkinetic model predicted 79% conversion with 81% selectivity toward formaldehyde at the lower temperature, increasing to a complete (100%) conversion with 73% selectivity at the higher temperature.

Machiels and Sleight (1982) studied methanol oxidation over $MoO_3 \cdot Fe_2(MoO_4)_3$ at lower temperatures in a continuous flow recycle reactor. They observed that the dependence of the reaction rate on the methanol partial pressure increases with temperature. According to their measurements, the reaction was 0.4 order in methanol at 435 K and 0.6 order at 524 K. The microkinetic model predicted the reaction order in methanol to change from 0.5 to 0.6 over this temperature range. Furthermore, these authors observed an inhibiting effect of water on the reaction rate. At 493 K, the reaction rate was found to be -0.9 order with respect to water, this phenomenon being attributed to competitive adsorption. In agreement with this result, the microkinetic model predicts the reaction to be negative first-order with respect to the water partial pressure.

The same authors also measured an oxygen order of 0.1 and an activation energy of 86 $kJ \cdot mol^{-1}$ for methanol oxidation. The microkinetic model predicts the reaction to be zero-order in oxygen, with an activation energy of 84 $kJ \cdot mol^{-1}$. Finally, from the reported rate of 10^{-6} mol CH_3OH converted per second per gram of catalyst and assuming a surface area of $10^4 m^2/kg$ (which is typical for these types of catalysts) and a site density of $10^{19}/m^2$, one can calculate a turnover frequency of $6 \times 10^{-3}\ s^{-1}$. This value differs only by a factor of two from the value of $1.4 \times 10^{-2}\ s^{-1}$ predicted by the microkinetic model for the same conditions.

Pernicone and coworkers (1969) studied methanol oxidation over a $[MoO_3 \cdot Fe_2(MoO_4)_3]$ catalyst in a plug flow reactor. Their results at 505 K showed the reaction to be 0.5 order in methanol at low methanol partial pressures, becoming zero-order when the methanol partial pressure was raised above 2.7×10^4 Pa. They also reported the reaction to be zero-order in oxygen and calculated an activation energy of 92 $kJ \cdot mol^{-1}$ for temperatures between 455 and 505 K. The microkinetic model predicted the reaction to be 0.6 order in methanol at low methanol partial pressures becoming 0.3 order near 2.7×10^4 Pa. Furthermore, the reaction rate was found to be independent of the oxygen partial pressure under the experimentally studied conditions. Finally, the simulations resulted in an activation energy of 88 $kJ \cdot mol^{-1}$.

The oxidation of carbon monoxide to carbon dioxide over V_2O_5/SiO_2 was studied by Goldwasser and Trimm (1979). At 733 K, they found the reaction to be first-order in CO and zero-order in oxygen. The microkinetic model gives the same results. Furthermore, in the temperature range of 673 to 773 K, the activation energy of the reaction was experimentally determined to be 105 $kJ \cdot mol^{-1}$, while the model predicts a slightly higher value of 132 $kJ \cdot mol^{-1}$.

Pitchai and Klier (1986) studied the effect of the water vapor on the performance of a $MoO_3/SiO_2 \cdot Al_2O_3$ catalyst during methane oxidation. The addition of water in the reactant mixture at 848 K resulted in a significant decrease in the activity of the catalyst. In addition, the presence of water favored the formation of formaldehyde at the expense of carbon monoxide, while the percentage of carbon dioxide remained virtually unchanged. When moved to the same conditions, the microkinetic model displayed the same qualitative trends.

Dowden and Walker (1971) combined high pressures (5.47×10^6 Pa) and a high methane to oxygen ratio (CH_4/O_2 = 98:2) to achieve high selectivities in methanol production during methane oxidation, e.g., 19% selectivity toward methanol at 2.3% methane conversion was observed over MoO_3. Under the same conditions, the microkinetic model does not predict the formation of any significant amounts of methanol. However, the model predictions can be improved by increasing the desorption rate constant of methanol or by increasing the hydroxyl coverage of the surface. The latter approach seems more promising. Specifically, the model predicts the hydroxyl coverage under these conditions to be approximately 95%, compared to coverages between 1 and 15% for the conditions of Spencer and Pereira. To achieve significant production of methanol, one would have to increase the hydroxyl coverage to levels above 99.5%. One could say, therefore, that while our model has captured the major changes in hydroxyl coverage, it does not necessarily describe in detail, by the use of a Langmuir equation, the pressure and temperature dependence of this hydroxyl coverage.

Microkinetic vs. Macrokinetic Considerations

As demonstrated previously, the microkinetic model of this study simulates well the activity and selectivity for methane, methanol, and formaldehyde oxidations over MoO_3/SiO_2 and V_2O_5/SiO_2 catalysts, under the conditions studied by Spencer and Pereira. These same authors also achieved agreement between simulated and experimentally observed kinetic data, using the following simpler macrokinetic model for MoO_3 and V_2O_5, respectively:

$$\begin{array}{ccccccc} & & & & R_1 & & R_2 \\ & & CH_4 & \rightarrow & CH_3OH & \rightarrow & HCHO \rightarrow CO \\ & R_3 \downarrow & & & \downarrow & & \\ & & CO_2 & & CH_3OCH_3 & & \end{array}$$

$$\begin{array}{ccccccc} & R_4 & & R_5 & & R_6 & \\ CH_4 & \rightarrow & HCHO & \rightarrow & CO & \rightarrow & CO_2 \end{array}$$

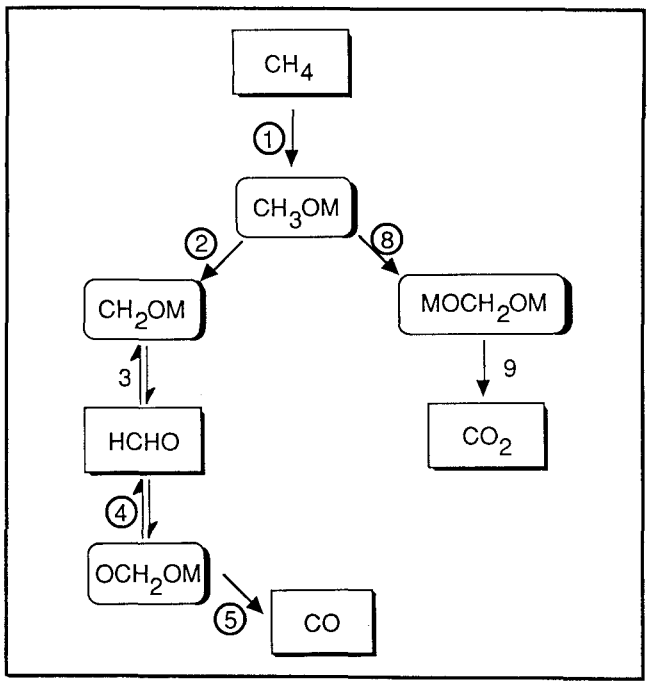

Figure 7a. Active steps in the microkinetic model for methane partial oxidation over MoO_3/SiO_2.

For comparison, the reaction steps active under those conditions according to the microkinetic model are given in Figures 7a and 7b.

The micro- and macrokinetic models are both based on the existence of two pathways for the formation of CO_2: one route directly from methane and the other through HCHO and CO.

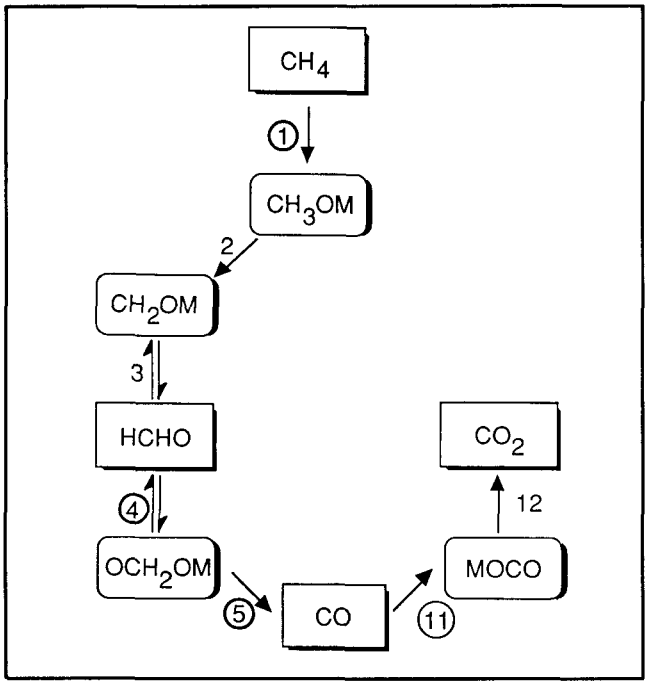

Figure 7b. Active steps in the microkinetic model for methane partial oxidation over V_2O_5/SiO_2.

Table 5. Turnover Frequencies of Corresponding Model Reactions for CH_4 Partial Oxidation over MoO_3/SiO_2*

	Macrokinetic Model			Microkinetic Model	
	873 K	923 K		873 K	923 K
R_1	4.8×10^{-2}	1.9×10^{-1}	r_2	4.5×10^{-2}	1.9×10^{-1}
R_2	3.5×10^{0}	9.5×10^{0}	r_5	3.4×10^{0}	6.7×10^{0}
R_3	5.8×10^{-3}	2.4×10^{-2}	r_8	8.1×10^{-3}	2.4×10^{-2}

*Units in s^{-1}, $P_{tot} = 1 \times 10^5$ Pa, 9:1 methane to oxygen molar ratio.

Furthermore, both models predict that the amount of CO_2 formed is nearly independent of the methane conversion level and the temperature, when MoO_3 is used as the catalyst. In the case of the microkinetic model, this is achieved by having both steps associated with the direct route (8 and 9) being irreversible and with a low Polanyi constant. The oxidation of CO to CO_2 appears to be insignificant under these experimental conditions over molybdena. The macrokinetic model achieves the same result by the use of the same activation energy for both the direct and the indirect routes, with a low preexponential factor associated with the direct route. No mechanistic step is present to account for any possible CO oxidation to CO_2.

The experimental results indicate that when V_2O_5 is used as the catalyst, CO_2 is a secondary product. In the microkinetic model, the differences in the bonding parameters between MoO_3 and V_2O_5 resulted in the suppression of the direct route in favor of the indirect pathway. On the contrary, a different network was proposed for the macrokinetic model when V_2O_5 was used as the catalyst, in which the direct route to CO_2 was eliminated and the CO oxidation step was added.

Examination of the micro- and macrokinetic models reveals that under the conditions studied by Spencer and Pereira, the microkinetic model can be reduced to the macrokinetic model. In the case of MoO_3, for example, the combination of steps 1, 2 and 3 of the microkinetic model results in the step labeled R_1 in the macrokinetic model. Similarly, the combination of steps 4 and 5 results in the step labeled R_2, and the combination of steps 1, 8 and 9 corresponds to the step labeled R_3. We now see that if step 1 of the microkinetic model is slow, then the use of a common activation energy for steps labeled R_1 and R_3 in the macrokinetic model can be justified. Our microkinetic simulations indeed show that step 1 is slow and irreversible under the studied conditions.

It is important to examine and compare the rates predicted by both models for the different steps of the process. In Table 5, the rates predicted by the macrokinetic model at 873 and 923 K over MoO_3 are given and compared with the rates of the corresponding irreversible steps 2, 5 and 8 of the microkinetic model under the same conditions. There is a good agreement between the two sets of rates, which explains why both models were able to simulate the experimental data well.

Similar observations can be made when V_2O_5/SiO_2 is used as the catalyst. A combination of steps 1, 2 and 3 of the microkinetic model results in the step labeled R_4 in the macrokinetic model, the combination of steps 4 and 5 corresponds to the step labeled R_5 and the combination of steps 11 and 12 results in the step labeled R_6. In Table 6, the rates of the macrokinetic model at 823 and 873 K are compared to those

Table 6. Turnover Frequencies of Corresponding Model Reactions for the CH_4 Partial Oxidation over V_2O_5/SiO_2*

	Macrokinetic Model			Microkinetic Model	
	823 K	873 K		823 K	873 K
R_4	7.1×10^{-2}	5.6×10^{-1}	r_2	1.4×10^{-1}	6.8×10^{-1}
R_5	1.4×10^{1}	3.6×10^{1}	r_5	1.4×10^{1}	1.9×10^{1}
R_6	5.7×10^{-1}	1.3×10^{0}	r_{11}	5.3×10^{-1}	1.6×10^{0}

*Units in s^{-1}, $P_{tot} = 1 \times 10^5$ Pa, 9:1 methane to oxygen molar ratio.

of the corresponding irreversible steps 2, 5 and 11 of the microkinetic model. The agreement is not as close as for the case of MoO_3; however, both models simulate adequately the experimental data.

Concluding Remarks

One of the objectives of this study was to determine whether a simple microkinetic model, using a limited number of physically meaningful parameters, could satisfactorily describe the network of methane, methanol, formaldehyde and carbon monoxide oxidation reactions over silica-supported molybdena and vanadia. The results show that this study has been successful in this respect. The proposed mechanism, although not necessarily complete or correct in detail, appears to have captured the essential chemistry of the processes and agrees with the existing literature.

We have compared the microkinetic model to the simpler macrokinetic described previously. Both models are successful in describing the methane partial oxidation data of Spencer and Pereira. The major advantage of the macrokinetic model is its simplicity. Its applicability, however, is limited to a rather narrow range of temperatures and pressures, since other experiments have shown that both the reaction orders and the activation energies change with reaction conditions (Pernicone et al., 1969; Machiels and Sleight, 1982). In addition, the macrokinetic model does not take into account effects of water vapor and has different reaction networks for molybdena and vanadia.

The microkinetic model also oversimplifies the surface catalytic chemistry; however, we have attempted to incorporate at least some of the essential aspects of the surface chemistry into the model. The major advantage of this model is its generality, demonstrated by its ability to explain experimental results of diverse nature from different sources. In addition, this model allows extrapolation to lower temperatures and correctly predicts methanol oxidation data, as well as variable kinetic orders. It has also captured the inhibiting effect of water vapor on the reaction rates. Thus, this microkinetic model provides a useful tool for extrapolating existing kinetic data over a wide range of experimental conditions and for linking the kinetics observed for methane activation with the oxidation kinetics for the subsequent gaseous intermediates involved in the catalytic process. As the microkinetic model is revised to describe more information available from diverse experimental measurements, it becomes a better tool for the design of new catalysts based on the fundamental principles of chemical kinetics. We hope that this article presents a first step in this direction for the partial oxidation of methane.

Notation

D_{O_2} = gas-phase dissociation energy of O_2
E_{A_i} = activation energy of step i of the microkinetic model
E_0 = Polanyi constant
$H_{f,i}$ = heat of formation of species i
K_i = equilibrium constant of step i of the microkinetic model
k_i = rate constant of step i of the microkinetic model
M=O = strength of bond between atomic oxygen and a surface metal atom
M-OCH_2 = strength of bond between a formaldehyde molecule and a surface metal atom
M-OCH_3 = strength of bond between a methoxyl group and a surface metal atom
M-OH = strength of bond between a hydroxyl group and a surface metal atom
MO-CH_2O = strength of bond between a formaldehyde molecule and a surface oxygen atom
MO-CO = strength of bond between a carbon monoxide molecule and a surface oxygen atom
Q_{O_2} = heat of adsorption of O_2
R_i = net rate of step i of the macrokinetic model
α = Polanyi constant
ΔH_{ads} = heat of adsorption
ΔH_i = heat of reaction of step i of the microkinetic model

Acknowledgment

Authors at the University of Wisconsin would like to acknowledge partial financial support from the Department of Energy.

Literature Cited

Busca, G., "On the Mechanism of Methanol Oxidation over Vanadia-Based Catalysts: a FT-IR Study of the Adsorption of Methanol, Formaldehyde and Formic Acid on Vanadia and Vanadia-Silica," *J. Mol. Catal.*, **50**, 241 (1989).

Cairati, L., P. Forzatti, F. Trifiro, and P. Villa, "Oxidation of Methanol in a Fluidized Bed: Fe_2O_3-MoO_3 and MoO_3 Supported on Silica," *Proc. Climax Int. Conf. on the Chemistry and Uses of Molybdenum*, Golden, CO, 402 (1982).

Chung, J. S., and C. O. Bennett, "On the Shift in the CH Stretching Bands of Methoxy Groups Chemisorbed on Metal Oxides," *J. Catal.*, **92**, 173 (1985).

Chung, J. S., R. Miranda, and C. O. Bennett, "Mechanism of Partial Oxidation of Methanol over MoO_3," *J. Catal.*, **114**, 398 (1988).

Chung, J. S., R. Miranda, and C. O. Bennett, "Study of Methanol and Water Chemisorbed on Molybdenum Oxide," *J. Chem. Soc., Faraday Trans. 1*, **81**, 19 (1985).

Dowden, D. A., C. R. Schnell, and G. T. Walker, "Creation of Complex Catalysts," *Proc. Int. Cong. on Catalysis*, Moscow, 201 (1968).

Dowden, D. A., and G. T. Walker, "Oxygenated Hydrocarbons by Gaseous-Phase Catalytic Oxidation," UK Pat. 1,244,001 (1971).

Edwards, J., J. Nicolaidis, M. B. Cutlip, and C. O. Bennett, "Methanol Partial Oxidation at Low Temperature," *J. Catal.*, **50**, 24 (1977).

Feil, F. S., J. G. van Ommen, and J. R. H. Ross, "Infrared Investigation of the Adsorption and Reactions of Methanol on V_2O_5/TiO_2 Catalysts," *Langmuir*, **3**, 668 (1987).

Goddard, S. A., M. D. Amiridis, J. E. Rekoske, N. Cardona-Martinez, and J. A. Dumesic, "Kinetic Simulation of Heterogeneous Catalytic Processes: Ethane Hydrogenolysis over Supported Group VIII Metals," *J. Catal.*, **117**, 155 (1989).

Goldwasser, M. R., and D. L. Trimm, "Oxidation of Carbon Monoxide on Vanadia," *Ind. Eng. Chem. Prod. Res. Dev.*, **18**(1), 27 (1979).

Kaliaguine, S. L., B. N. Shelimov, and V. B. Kazansky, "Reactions of Methane and Ethane with Hole Centers O^-," *J. Catal.*, **55**, 384 (1978).

Khan, M. M., and G. A. Somorjai, "A Kinetic Study of Partial Oxidation of Methane with Nitrous Oxide on a Molybdena-Silica Catalyst," *J. Catal.*, **91**, 263 (1985).

Klier, K., "Methanol Synthesis," *Advances in Catalysis*, 31, Academic Press, New York (1982).

Klissurski, D. G., "The Reactivity of Oxygen in Metal Molybdates," *Proc. Climax Int. Conf. on the Chemistry and Uses of Molybdenum*, Ann Arbor, MI, 123 (1979).

Ko, E. I., and R. J. Madix, "Reactions of Formaldehyde and Methanol on Clean, Carburized and Oxidized Mo(100) Surfaces," *Surf. Sci.*, **112**, 373 (1981).

Krivanek, M., P. Jiru, and J. Strnad, "Adsorption and Heat of Adsorption of Propylene on a Bi-Mo Oxide Catalyst," *J. Catal.*, **23**, 259 (1971).

Machiels, C. J., and A. W. Sleight, "A Kinetic Study of the Oxidation of Methanol over Molybdate Catalysts," *Proc. Climax Int. Conf. on the Chemistry and Uses of Molybdenum*, Golden, CO, 411 (1982).

Muzykantov, V. S., P. Jiru, K. Klier, and J. Novakova, "Exchange Reaction of Oxygen with Oxides. Computer Determination of the Exchange Rates," *Coll. Czech. Chem. Commun.*, **33**, 829 (1968).

Pankratiev, Y. D., L. N. Kurina, T. V. Lazareva, and S. P. Rabota, "Activity and Bond Strength of Surface Oxygen in Vanadium Oxide Catalysts for Methanol Oxidation," *React. Kinet. Catal. Lett.*, **27**(1), 173 (1985).

Pernicone, N., F. Lazzerin, G. Liberti, and G. Lanzavecchia, "On the Mechanism of CH_3OH Oxidation to CH_2O over MoO_3-$Fe_2(MoO_4)_3$ Catalyst," *J. Catal.*, **14**, 293 (1969).

Pitchai, R., and K. Klier, "Partial Oxidation of Methane," *Catal. Rev.-Sci. Eng.*, **28**(1), 13 (1986).

Shustorovich, E., "Chemisorption Phenomena: Analytic Modeling Based on Perturbation Theory and Bond-Order Conservation," *Surf. Sci. Reports*, **6**, 1 (1986).

Spencer, N. D., "Partial Oxidation of Methane to Formaldehyde by Means of Molecular Oxygen," *J. Catal.*, **109**, 187 (1988).

Spencer, N. D., and C. J. Pereira, "Partial Oxidation of CH_4 to HCHO over a MoO_3-SiO_2 Catalyst: A Kinetic Study," *AIChE J.*, **33**, 1808 (1987).

Spencer, N. D., and C. J. Pereira, "V_2O_5-SiO_2-Catalyzed Methane Partial Oxidation with Molecular Oxygen," *J. Catal.*, **116**, 399 (1989).

Sperber, H., "Manufacture of Formaldehyde from Methanol at BASF," *Chem. Ing. Tech.*, **41**, 962 (1969).

Stradella, L., and G. Vogliolo, "Energetics of the Adsorption of Propene, Water, Dioxygen on Bismuth Molybdate (2:1)," *Z. Phys. Chem. NF*, **137**, 99 (1983).

Van Hook, J. P., "Methane Steam Reforming," *Catal. Rev.-Sci. Eng.*, **21**, 1 (1980).

Manuscript received June 26, 1990, and revision received Nov. 14, 1990.